ACS Catalysis

Research Article

pubs.acs.org/acscatalysis

Olefin Metathesis by Grubbs–Hoveyda Complexes: Computational and Experimental Studies of the Mechanism and Substrate-Dependent Kinetics

Ian W. Ashworth,[†] Ian H. Hillier,*[,‡] David J. Nelson,[§,∥] Jonathan M. Percy,*[,§] and Mark A. Vincent[‡]

[†]Global Research and Development, AstraZeneca, Silk Road Business Park, Charter Way, Macclesfield SK10 2NA, U.K.

[‡]School of Chemistry, University of Manchester, Oxford Road, Manchester M13 9PL, U.K.

[§]WestCHEM, Department of Pure and Applied Chemistry, University of Strathclyde, 295 Cathedral Street, Glasgow G1 1XL, U.K.

Supporting Information

ABSTRACT: The potential energy surfaces for the activation of Grubbs–Hoveyda-type precatalysts with the substrates ethene, propene, 1-hexene, and ethyl vinyl ether (EVE) have been probed at the density functional theory (DFT) (M06-L) level. The energetically favored pathway of the reaction leading to a 14e Fischer carbene and styrene starts with an initiation step in which the incoming substrate and outgoing alkene ligand are both clearly associated with the ruthenium center. For these substrates, with the exception of ethene, the rate determining step is predicted to be the formation of the metallocyclobutane (MCB). We have taken the initial reactant to be a weak van der Waals complex between substrate and precatalyst. This model yields good agreement between the computed activation parameters for both the parent Grubbs–Hoveyda and Grela complex with EVE substrate, and the experimental values, reported here. The alternative model which takes the initial reactant to be two isolated molecules requires an estimate of the entropy loss on formation of the initial complex in solution which is difficult to evaluate. Our estimate of this quantity yields a barrier for the rate determining step for the interchange mechanism which is close to the value we find for the alternative mechanism in which the rate determining step is the initial dissociation of the precatalyst. The relative energetics of these two mechanisms involving different initiation steps but with similar activation barriers, could well be dependent upon the precatalyst and substrate in line with the recent experimental findings of Plenio and co-workers.

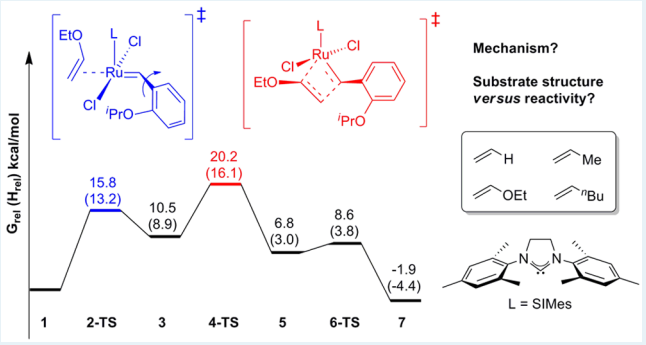

KEYWORDS: *olefin metathesis, reaction mechanism, potential energy surface, Grubbs–Hoveyda type complexes, Fischer carbene, density functional theory, kinetic studies*

INTRODUCTION

Olefin metathesis by ruthenium carbenes is a powerful tool for the formation of C–C bonds in a wide variety of chemical situations,[1,2] with both experimental and computational studies making our understanding of the mechanism of these catalysts increasingly more quantitative.[3−6] Experimental and computational studies of the first- and second-generation Grubbs catalysts (**G1** and **G2**) have established that dissociation of the phosphine ligand (PCy_3) is the rate determining step, with estimates of the free energy difference between precatalyst and active 14e catalyst being in the range 18–26 kcal mol^{-1},[7−9] the subsequent steps in the mechanism being predicted to be significantly exergonic with respect to this 14e species.

Because of research by a variety of groups, a considerable number of metathesis precatalysts are now known.[10,11] Until recently, it had been assumed that other classes of metathesis catalyst of the form [RuX_2 (L)(L′)=CHR] (where X is a halide or pseudohalide, L is a phosphine or NHC, and L′ is a dissociating ligand such as a phosphine, pyridine, or chelating ether) initiated in the same manner.[12]

However, for the Hoveyda-type class of catalyst (GH2),[13−15] there is kinetic evidence that the olefin itself is involved in the catalyst initiation step.[5,16−18] This has led to the suggestion that initiation involving association of the ligand, or rupture of the Ru–O bond coupled with binding of the ligand (interchange), rather than just rupture of the Ru–O bond (dissociation), is the favored initiation step. An experimental study by Plenio et al.[17] found that the initiation step may be dependent upon the nature of the substrate, and for some substrates it was suggested that both dissociative and interchange mechanisms may operate simultaneously and competitively. In a preliminary computational study of the initiation step in GH2 precatalysts, we have found that with ethene as the substrate, an interchange

Received: March 1, 2013
Revised: July 4, 2013
Published: July 12, 2013

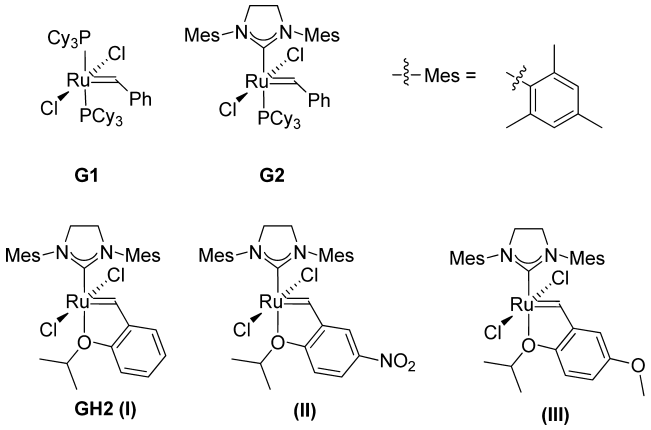

mechanism is favored, but that subsequent steps in the mechanism proceed with barriers that are only slightly lower than that of the interchange step.[5] We also found that a mechanism in which the olefin forms a six-coordinate intermediate with the Ru complex (association) was less favorable than an interchange mechanism. Calculations with ethyl vinyl ether as the substrate were in agreement with measured activation parameters from UV/visible spectroscopy experiments. In the search for improved performance, new families of Grubbs–Hoveyda catalysts continue to be developed,[13,19] and often reveal unexpected structure–activity relationships. For example, catalysts incorporating a chelating iodo-benzylidene ligand have shown intriguing substituent effects which suggest that the rate-determining step does not involve Ru···I–Ar bond breaking.[19]

Theoretical investigations of the underlying mechanisms are therefore timely and important, and complement key results obtained from experimental studies over the past 2–3 years. A thorough understanding of the initiation step in any catalytic cycle is essential to inform future efforts to optimize or tune the process which delivers active species into the catalytic cycle itself.

Thus, a quantitative understanding of the potential energy surface (PES), particularly an understanding of which step is rate determining, as well as the interplay between precatalyst and substrate structure and reactivity, are essential to provide insights which can be used by organometallic chemists to design new and more effective catalysts. These considerations have led to this computational study where we focus on the effect of different substrates on the PES of the catalytic reaction, particularly those studied experimentally by Plenio et al.[17] and of related modified catalysts. We have studied three such Ru complexes, the Grubbs–Hoveyda complex (GH2, **I**), the Grela

Scheme 1. Reaction Pathways for Olefin Metathesis

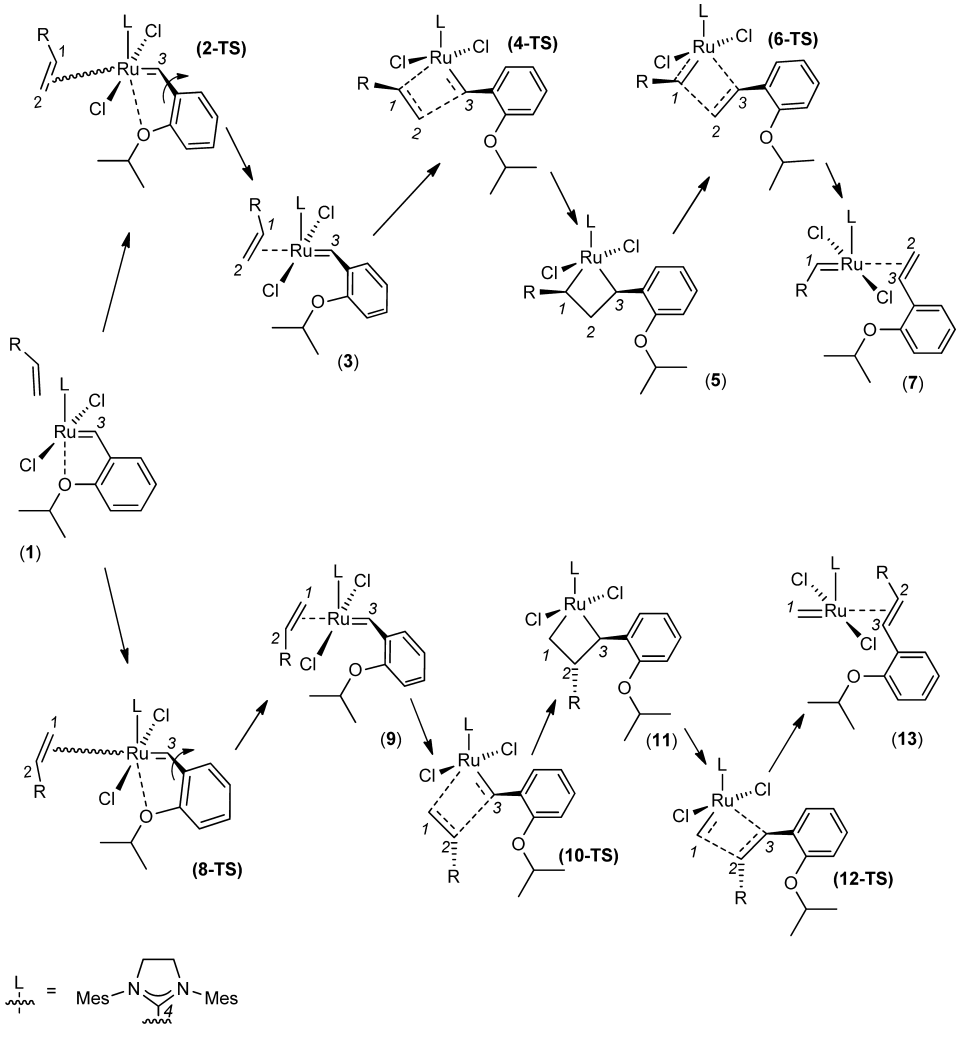

dx.doi.org/10.1021/cs400164w | ACS Catal. 2013, 3, 1929–1939

complex (**II**), and (**III**), where OMe replaces NO_2 in (**II**). We have modeled (**III**), for although it is not a commercial catalyst and we have not studied it experimentally, it provides a comparison of an electron donating group (OMe) with the electron withdrawing group (NO_2) found in the Grela complex (**II**).

COMPUTATIONAL DETAILS

We have used density functional theory (DFT) employing the M06-L functional[20−22] to study the PES for the reaction in Scheme 1, in which initiation of the precatalyst (**1**) occurs by either a dissociative or interchange mechanism and leads to the Dewar−Chatt−Duncanson η^2-complex (**3**). We have chosen this functional since weak intermolecular interactions which may be present in these systems are well described by the M06 class of functional.[23,24] Structures were optimized using a basis set previously denoted B2[4] which consists of the SDD ECP and corresponding basis on Ru, with additional f-functions, and with a 6-311G** basis on all other atoms. The thermodynamic corrections (at 298.15 K) were obtained from structures optimized with a somewhat smaller basis previously denoted B1.[4] Solvation was included using the C-PCM model with a dielectric of 8.93 (dichloromethane), and we quote both free energies and enthalpies including the solvation free energy, at a standard state of 1 M solution. All calculations were carried out using Gaussian 09.[25]

We take the reactant to be a weak van der Waals complex of precatalyst and substrate. There may be a number of such structures for each substrate, and we here consider the reactant structure to be the one that connects to the transition structure (**2-TS**) involved in the formation of the η^2-complex (**3**). The next step is the formation of the metallacyclobutane (MCB) (**5**) by a [2 + 2] cycloaddition via **4-TS**, followed by a retro [2 + 2] via **6-TS** to yield the alkylidene product bound as a η^2-complex (**7**). We note that for the simplest substrate ethene, only one alkylidene can be formed. However, for nonsymmetric substrates, there are two alternative pathways that lead to either methylidene itself (**13**) or a more substituted alkylidene (**7**), as product. There are four possible orientations of the substituted ethenes in the η^2-complex corresponding to the 4 positions of substitution of ethene (Scheme 2). Out of the 4 corresponding

Scheme 2. Possible Orientations of the Substituted Ethenes in the η^2-Complex (3), (9)

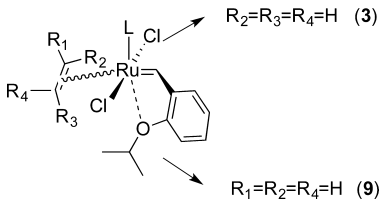

TSs leading to these η^2-complexes we have chosen the two which are considered to be the least sterically crowded (Scheme 1), and these lead to MCB(**5**) and MCB(**11**) having cis and trans configurations respectively.

To complement this computational study we report experimental rate parameters measured for an ethyl vinyl ether (EVE) substrate. Time dependent UV/visible spectroscopy was used to follow the reaction of **I** and **II** with EVE, using the decrease of the signal at λ_{max} = 375 nm, which is taken to be due to metal-to-ligand charge transfer (MLCT) into the π^* orbital of the Ru=CHR bond.[3,26] To identify which steps in the mechanism are being monitored in this way, we have used time dependent DFT (TD-DFT) calculations with basis B1 to follow the change in this absorbance across the PES. We have here used the hybrid exchange-correlation functional CAM-B3LYP[27] having improved long-range properties compared to B3LYP. This functional has been widely used to model excited states.[28]

COMPUTATIONAL RESULTS

Dissociative Initiation. We first discuss the dissociative initiation mechanism for the three precatalysts studied. We have identified two TSs of similar energies, which we label **14-TS** and **15-TS**; the computed energetics are shown in Table 1, and the structures are indicated in Scheme 3.

Table 1. Standard State Free Energies and Standard State Enthalpies for Dissociative Initiation of I−III[a]

precatalyst	$\Delta G^{0‡}$ (kcal mol^{-1})	$\Delta H^{0‡}$ (kcal mol^{-1})
I	24.0 (22.6)	24.6 (22.8)
II	23.2 (21.4)	23.3 (21.5)
III	24.7 (20.9)	24.3 (23.0)

[a]The values are for **14-TS**, and, in parentheses, for **15-TS**.

Scheme 3. Dissociative Transition Structures (14-TS), (15-TS)

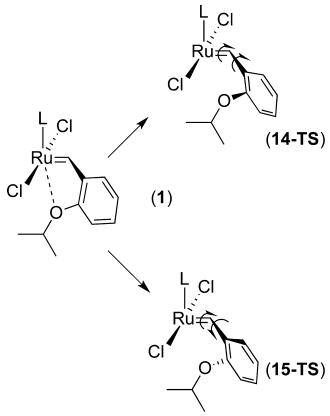

The key bond distances and angles from the corresponding stationary structures are shown in Supporting Information, Table S1. We see an elongation of the Ru−O distance of ∼1 Å in these structures, resulting from internal rotation around the ruthenium/alkylidene Ru=C bond, thus decreasing the C^4−Ru=C^3−C^{Ar} dihedral angle from a value close to 180° in the reactants, to ∼155−175° in the TSs, the two structures differing in the direction of the rotation about C3−C. We find that our lower energy structure (**15-TS**) is similar to that found by Solans-Monfort et al.[29] The computed barriers for each TS are within 1 kcal mol^{-1} for all three precatalysts, and there are also only small differences in the predicted geometries of the corresponding reactants and TSs. As expected, the corresponding entropies of activation are small and positive (∼2 cal K^{-1} mol^{-1}). The well-documented electron withdrawing effect of the NO_2 group[14,15] leads to a slightly elongated Ru−O distance in the reactant, and a correspondingly small reduction in the reaction barrier. The electron donating effect of the OMe group is less evident, with essentially no change in the structures of the reactant or TS. We do find the expected small increase in

dx.doi.org/10.1021/cs400164w | ACS Catal. 2013, 3, 1929−1939

the free energy barrier, although the enthalpic barrier is slightly lowered.

Interchange Mechanism. We now seek to identify the role of the different substrates in determining the structural and energetic aspects of the reaction mechanism, and first discuss some general aspects of the predicted PES. We note first that the structural changes as the reaction proceeds are similar at a semiquantitative level for the different substrates, as shown in Supporting Information, Table S2. As in the dissociative initiation mechanism, the initiation step for the interchange mechanism requires a considerable extension of the Ru−O distance, and here leads to a reduction in the C^4−Ru═C^3−C^{Ar} angle from ∼180° to ∼145°. We thus find that the extent of rotation of the alkylidene is less in the dissociative than in the interchange mechanism, shown in Figure 1, which is somewhat

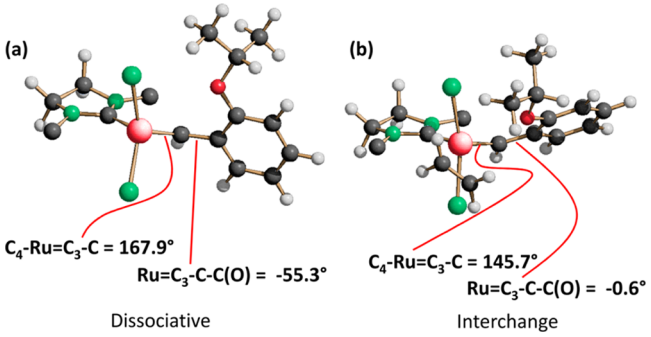

Figure 1. Transition structures for the initiation of precatalyst **I** via (a) a dissociative mechanism (**14-TS**) and (b) an interchange mechanism with ethene; the mesityl groups have been omitted for clarity.

unexpected. The associated elongation of the Ru−O distance is in the range 0.6−0.8 Å for the interchange mechanism, but is considerably greater at ∼1.1 Å for the dissociative mechanism. The greater Ru−O distance for dissociation stems from a small change in the C−Ru═C−C dihedral together with rotation about the C−C3 bond (see Scheme 1 for atom labeling). In the interchange mechanism the alkylidene rotates sufficiently to permit the alkene to bind, while the corresponding dissociative mechanism is via **14-TS** and involves an unfavorable steric interaction between the iso-propyl ether group and a Cl ligand. These geometry changes have very little effect on the Ru═C and alkene double bonds, with the Ru−C3 and C1−C2 bonds lengths in **2-TS** being essentially unchanged from their values in the initial weak substrate-catalyst complex. The formation of the η^2-complex (**3**) from **2-TS** results in a reduction of the two Ru−C(alkene) distances by up to 1 Å, a definite increase in the C1−C2 length of up to 0.03 Å, and an elongation of the Ru−Cl bonds of up to 0.07 Å. The [2 + 2] cycloaddition to form the MCB intermediate (**5**) via **4-TS**, requires further rotation of the phenyl ether to allow the alkene to approach the alkylidene. In **4-TS** the Ru−C distances are midway between those of the η^2-complex (**3**) and MCB (**5**), with a small reduction in the lengths of the two new Ru−C bonds, and a corresponding increase in the Ru−C3 length. The subsequent opening of the MCB to give the alkylidene takes place via a TS (**6-TS**) similar to that involved in its formation (**4-TS**) having, as expected a longer Ru−C3 and a shorter Ru−C1 distance compared to **4-TS**. We note that the length of the C1−C2 bond in the MCB, which is broken to form the final η^2-complex, varies from 1.57 Å for ethene to 1.65 Å for EVE and reflects the ease with which the final η^2-complex (**7**) is formed. The final step in the reaction sequence is the dissociation of the η^2-complex (**7**) to give a 14e ruthenium species and the alkylidene.

Ethene, Propene, and 1-Hexene Substrates. We now examine in more detail how the PESs are dependent upon the identity of the substrate. For ethene, we see from Figure 2 that

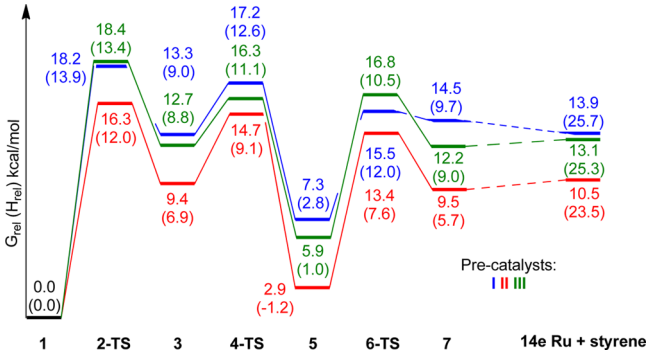

Figure 2. PES for the metathesis of ethene by precatalysts **I** (**blue**), **II** (**red**), and **III** (**green**); standard state free energies are provided, with enthalpies in brackets (kcal mol^{-1}).

the most stable intermediate species is the MCB (**5**). However, all three TSs leading to the formation of the final η^2-complex are within 3 kcal mol^{-1} so that it is likely that their relative ordering could well be sensitive to changes in the substrate and/or catalyst structure. We note that the barrier computed for both initial dissociative steps (Table 1) are greater by 4−7 kcal mol^{-1} than for an interchange mechanism, so that it is likely to remain the less favored pathway with only modest changes in substrate or catalyst structure. Notably, methylidene plus styrene is energetically uphill from the precatalyst in each case, by 10−14 kcal mol^{-1}. The less electron rich styrene (bearing the nitro functionality) reduces this energetic difference. These results are in agreement with the results of Schore and co-workers who measured equilibrium constants for the reaction of **G1** with a number of alkenes and concluded that more electron-rich alkylidenes were formed more favorably.[30]

Attempts were made to explore the initiation of complex **I** with ethene experimentally, using ^{1}H NMR spectroscopy. Ethene-sparged chloroform-*d* was added to solid internal standard (1,3,5-trimethoxybenzene) and **GH2** (ca. 2.6 mmol L^{-1}) in an NMR tube at 293 K and the concentration of **GH2** was monitored over time by ^{1}H NMR integration (Figure 3); the initial concentration of ethene was found to be 63 mmol L^{-1}. In contrast to reactions with ethyl vinyl ether, the reaction

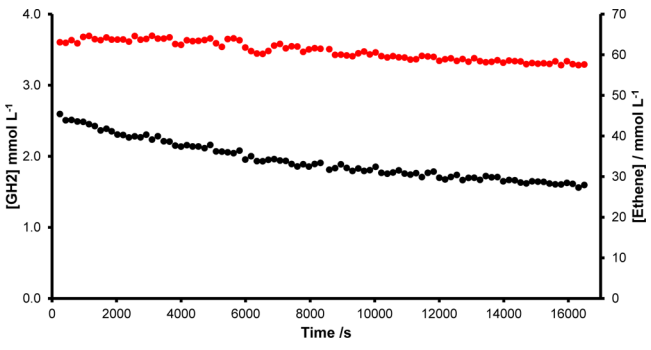

Figure 3. Reaction of **GH2** with ethene at 293 K showing the change in concentration of **GH2** (**black**) and ethene (**red**).

dx.doi.org/10.1021/cs400164w | *ACS Catal.* 2013, 3, 1929−1939

here was very slow, and reached only about 40% conversion in 5 h, consistent with the unfavorable equilibrium in operation.

We now consider the effect of changes to the precatalyst on the structure and energetics of the formation of the initial η^2-complex. There is a small reduction (1.9 kcal mol^{-1}) in the barrier for NO_2 substitution and a slight increase (0.2 kcal mol^{-1}) in its value for OMe substitution, with the lengthening of the Ru−O distance in the corresponding TSs being within 0.02 Å of each other. The effects of both the electron withdrawing and donating groups on **2-TS** are thus quite small. We have already noted a similar trend for the dissociative mechanism with the effect of OMe and NO_2 substitution on both the structure and the energetics of (**14-TS**) again being small although the donor effect of a methoxy through a π-system is expected to be quite large.[31]

The other steps in this reaction sequence that lead to the formation of the η^2-bound former alkylidene are of lower energy than the initiation step. Thus, for all three precatalysts the initial interchange reaction leading to the formation of the η^2-complex is rate determining, and the most stable intermediate is the MCB (**5**), although it is above the initial minimum. However, for Grela (**II**) the enthalpy of the MCB relative to the reactants is negative, and is positive by only 1 kcal mol^{-1} for **III**.

The initiation of **I** by the slightly larger alkene, propene (Figure 4), differs in one important aspect from ethene, since

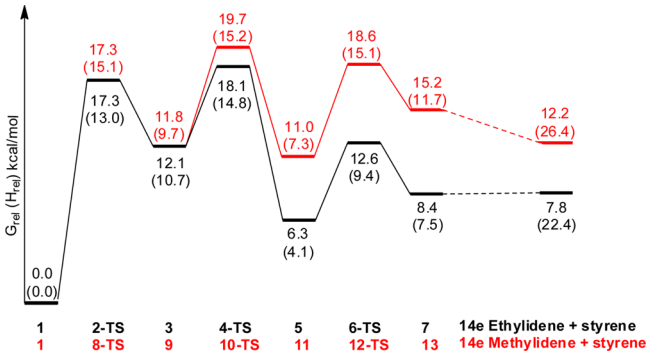

Figure 4. PES for the metathesis of propene by precatalyst **I**, either to yield a 14e ethylidene (**red**) or 14e methylidene complex (**black**); standard state free energies are provided, with enthalpies in brackets (kcal mol^{-1}).

differing orientations of the unsymmetrical substrate with respect to the Ru center lead to different structures for the η^2-complex (**3**) and subsequent structures along the pathway (see Scheme 1). We have considered two possible orientations of the substrate, which lead to different products (**7**,**13**), the corresponding TSs for the initial attack of the substrate leading to the two possible η-complexes being shown in Figure 5.

The activation energy of this step is found to be the same for both orientations of the attacking propene, and to be a little lower (by 0.9 kcal mol^{-1}) than for the less bulky ethene, which is somewhat surprising. For both ethene and propene substrates the TSs for the first two steps are within about 1 kcal mol^{-1} and are significantly greater than the barrier for MCB opening leading to the substituted methylidene (**7**) in the case of propene. For ethene it would appear that the formation of the initial η^2-complex is rate determining while for propene the second step to form the MCB via both conformations is somewhat higher than the first. In the case of propene it is the formation of the second η^2-complex (**7** or **13**) which shows the greatest difference in the energetics for the two substrate orientations. Thus, the energy of the TS for the opening of the MCB is significantly lower when the substituted methylidene (**5**→**7**), rather than the unsubstituted methylidene (**11**→**13**) is formed, the free energies of the TSs with respect to reactants being 12.6 and 18.6 kcal mol^{-1} respectively. The difference in these values is attributed to the relative stabilities of the two possible η^2-complexes (**7**, **13**), the one leading to the formation of the ethylidene (**7**) being considerably more stable (by ca. 7 kcal mol^{-1}), and is similarly more stable than the corresponding complex involving ethene. A number of MCBs which closely resemble **5** and **11** have been studied using low-temperature NMR techniques.[32−37] Literature precedent strongly suggests that MCBs of the type **11** are higher in energy than those of type **5**, in agreement with the calculations we present here.

For both ethene and propene substrates, we were unable to locate a TS corresponding to dissociation of the styrene from (**7**). We have however located transition structures with free energy barriers close to 5 kcal mol^{-1} which correspond to rotation of the alkylidene ligand, and in which the η^2-bond is considerably lengthened. These transition structures lead to minima where the alkylidene ligand is rotated by approximately 180° compared to (**7**), and the styrene ligand is rebound. If we take the final product to consist of two isolated molecules, their free energy is considerably lower than the corresponding enthalpy because of entropic contributions. In the case of EVE, for which we report experimental data, we have also considered a van der Waals product complex (vide infra).

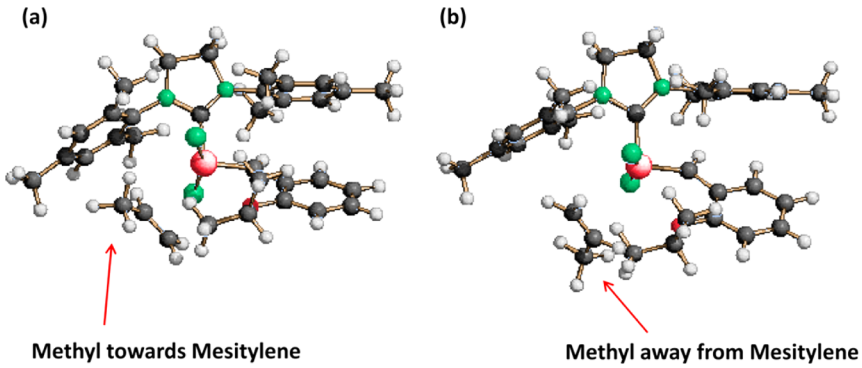

Figure 5. Transition structures for formation of initial η^2-complex with propene (a) via **2-TS** with the methyl group orientated toward the mesityl ring and (b) via **8-TS** with the methyl group orientated away from the mesityl ring.

dx.doi.org/10.1021/cs400164w | *ACS Catal.* 2013, 3, 1929−1939

The reported kinetic study employing 1-hexene as a substrate[17] has led us to carry out some limited calculations using this substrate, where it might be expected to have similar kinetic behavior to propene (Figure 6). We have studied the

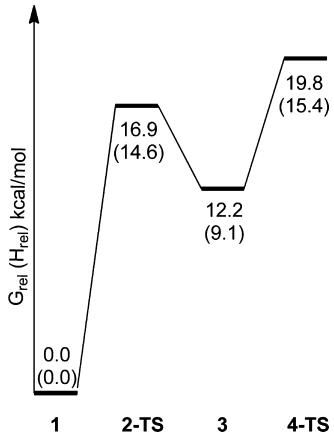

Figure 6. Partial PES for the metathesis of 1-hexene by precatalyst **I**; standard state free energies are provided, with enthalpies in brackets (kcal mol^{-1}).

PES up to the formation of the MCB, which in view of our results for propene is expected to contain the rate determining step. We found that in the two transition structures **2-TS** and **4-TS** the substrate adopts a coiled conformation which allows the bulky ^{n}Bu moiety to pass between the *iso*propyl ether group and a mesitylene methyl group in **2-TS**. It appears that this does not incur an energetic penalty, with **2-TS** being slightly lower than for propene, while **4-TS** is about 2 kcal mol^{-1} higher.

Ethyl Vinyl Ether Substrate. We now consider the reaction of EVE, which has frequently been studied experimentally and which has been used ubiquitously for the measurement of precatalyst initiation rates. As in the case of propene we have considered two orientations of the attacking substrate, one with the OEt group close to one of the aromatic rings of the *N*-heterocyclic carbene ligand (**3**) and one where it is pointing away from the ligand (**9**) (Figure 7 (**a**) and (**b**) respectively). We first note that for the three precatalysts studied here, despite the increase in size of the alkene, the initial binding of the substrate via **2-TS** has a lower barrier than for ethene, or propene in the case of **I**. The structures of **2-TS** for both pathways resulting in the first η^2-complex have considerably longer Ru−C1 and Ru−C2 distances than in the case of both ethene and propene, so that they are earlier than for ethene, both in terms of energetics and structure. This reflects the increased Lewis basicity of EVE compared to ethene, arising from the conjugation of the oxygen lone pairs with the alkene bond. For precatalysts **I**−**III** the transition structures having the OEt group directed away from the mesitylene ring (**8-TS** (**1**→**9**)) are always lower in energy than when this group is directed toward this ring (**2-TS** (**1**→**3**)). This may be understood in terms of the steric crowding expected with a group of the size of the ethoxy moiety.

Considering the second and third steps of the reaction sequence, it can be seen that for **I**−**III** the second step is always the most energetic, with more energy being required to form the MCB than to break it open. This can be associated with the conjugation of the oxygen lone pair into the alkene bond, present in the isolated substrate, but lost upon MCB formation.

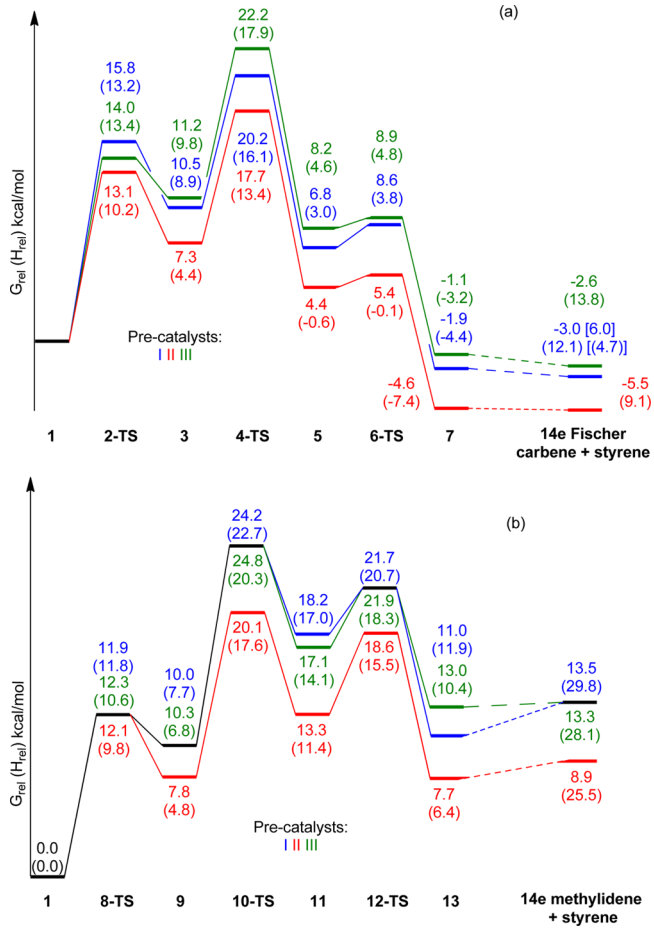

Figure 7. PES for the metathesis of ethyl vinyl ether by precatalysts **I** (**blue**), **II** (**red**), and **III** (**green**) to yield either (a) Fischer carbene or (b) methylidene; standard state free energies are provided, with enthalpies in brackets (kcal mol^{-1}). In (a), the values in square brackets are for a van der Waals complex.

This interaction is not present in ethene and hence for this substrate the energies of **4-TS** and **6-TS** are quite close. We also see that for EVE, **6-TS** which leads to a substituted alkylidene is of considerably lower energy than the alternative structure **12-TS**, a scenario we also observed for propene, which here reflects the stable Fischer carbene which forms from **6-TS** but not from **12-TS**. In addition we note that the barrier to the formation of these carbenes from the MCB is quite small, being less than 2 kcal mol^{-1}. As in the case of ethene and propene, we have not located a barrier for dissociation of the η^2-complex (**7**), but have located a low energy TS corresponding to rotation of the Fischer carbene ligand. We find that the final dissociation products when modeled both as individual molecules or as a van der Waals complex are considerably lower in both free energy and enthalpy than the highest energy transition structure, corresponding to the formation of the MCB (**5**). Thus, in the case of EVE for which experimental data exist, it is clear that the formation of the MCB is the rate determining step.

Our experimental rate data yield activation free energies of 19.6 and 18.2 kcal mol^{-1} respectively for precatalysts **I** and **II** (Table 2). We see that these values are in excellent agreement with the calculated barriers of the rate determining step, the formation of the MCB (**5**). The enthalpic and entropic contributions show similar excellent agreement between theory

dx.doi.org/10.1021/cs400164w | *ACS Catal.* 2013, 3, 1929−1939

Table 2. Experimental and Computed Energies for the Reaction of EVE with Pre-Catalysts I and II

	$\Delta G^{\ddagger}$ /kcal mol^{-1}		$\Delta H^{\ddagger}$ /kcal mol^{-1}		$\Delta S^{\ddagger}$ /cal K^{-1} mol^{-1}	
precatalyst	exp.	calc.	exp.	calc.	exp.	calc.
I	19.6	20.2	14.1	16.1	−18.5	−13.8
II	18.2	17.7	12.4	13.4	−19.3	−14.4

and experiment. The initial interchange step leading to the formation of the η^2-complex (**3**) is predicted to have considerably lower barriers for all three precatalysts, and shows a small reduction upon NO_2 substitution.

For 1-hexene, we find that the barrier for MCB formation (**4-TS**), 19.8 kcal mol^{-1}, is essentially the same as that computed for EVE, in line with the experimental finding of Plenio et al.[17] that both EVE and 1-hexene react at a similar rate. Examination of the structural parameters of **4-TS** for EVE and 1-hexene (Supporting Information, Table S2) reveals the close similarity displayed in Figure 8. In particular we see that the slightly longer hexene chain does not show different interactions with the ruthenium ligands compared to EVE.

The UV/visible spectrum of **I** exhibits an absorbance maximum at about 375 nm in the absence of substrate; in the presence of EVE this band is observed to decrease over time without an observable change in the shape of the absorbance band (Supporting Information, Figure S1). In parallel with the loss of this band, a new band at ∼300 nm grows in intensity. The spectrum clearly shows isosbestic points, indicating direct conversion between two species during the course of the reaction. We may use our TD-DFT calculations (Table 3) of the excited states of the minimum energy structures along the PES for the reaction of EVE with **I** to assign this spectrum. We predict a broad intense band with maxima at 365 and 354 nm respectively for the van der Waals (**1**) and the η^2-complex (**3**). For the van der Waals complex this state arises from orbital transitions from chlorine lone pair and metal d orbitals into vacant metal d and alkylidene carbon p orbitals. For the MCB (**5**), a strong peak is predicted at 350 nm and less strong peaks at 315 and 301 nm. It is only when the final η^2-complex (**7**) is reached that the intense band near 350 nm finally disappears and is replaced by a strong band at 282 nm, because of transitions between π orbitals on the η- ligand,

Table 3. TD-DFT Calculations of the Excited States for GH2 (I)/EVE Structures

structure	energy (eV)	λ (nm)	oscillator strength
1	3.26	380	0.06
	3.39	365	0.15
	3.41	363	0.02
	4.24	292	0.04
3	3.24	383	0.01
	3.50	354	0.22
	4.12	301	0.03
	4.20	295	0.04
5	3.54	350	0.12
	3.81	326	0.01
	3.93	315	0.07
	4.12	301	0.11
7	3.78	328	0.01
	3.93	315	0.06
	4.40	282	0.11

with some metal d character. Thus, using these predicted peak positions in conjunction with our calculated PES (Figure 7), we can assign the initial band to the complex of the precatalyst and weakly bound substrate, and possibly the initial η^2-complex (**3**), although the concentration of this latter species is likely to be small. In view of the low barrier for decomposition of the MCB(**5**), the concentration of this species is likely to be very small, and we thus assign the band at ∼300 nm to the final η^2-complex (**7**).

Alternative Pathways. The calculations presented so far have yielded a quantitative explanation of our observed kinetics for the EVE substrate. These calculations were based upon two of the four possible TSs leading to the formation of the initial η^2-complex. In view of our finding that the formation of **4-TS** is rate determining, we have examined in the case of Grela (**II**), the formation of the alternative **4-TS** for EVE which leads to the trans, rather than the cis configuration of MCB (**5**). Somewhat surprisingly this TS was only 6.2 kcal mol^{-1} above the initial van der Waals complex (**1**), which is considerably lower than the TS at 17.7 kcal mol^{-1} above (**1**) which leads to the cis configuration (Figure 7). In the interchange mechanism leading to the cis MCB, the formation of **4-TS** is a relatively

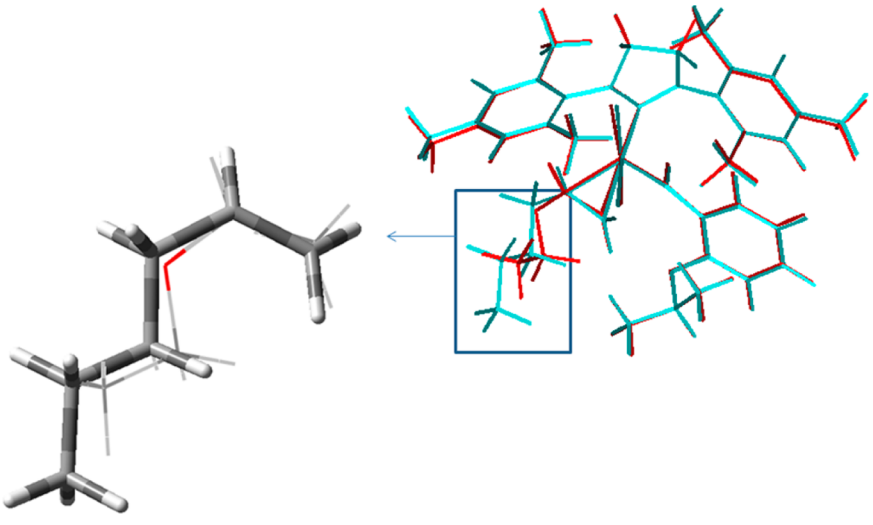

Figure 8. Overlay of **4-TS** for EVE and 1-hexene, with inset highlighting the OEt and "Bu moieties.

dx.doi.org/10.1021/cs400164w | ACS Catal. 2013, 3, 1929−1939

high energy process because of the steric interaction of the EVE which forces rotation of the phenyl ether. In contrast, in the alternative low energy TS the steric interaction is absent, this rotation having already occurred. This was shown by deletion of the EVE substrate from the low energy η-complex, and optimizing of the remaining 14e Ru complex, which led to the dissociated catalyst rather than the precatalyst. This low energy transition structure leads to an MCB (**5***) and η^2-complex (**3***) (Figure 9, with the $-NO_2$ group omitted) with correspondingly low energies of −1.4 and 4.1 kcal mol^{-1} with respect to (**1**).

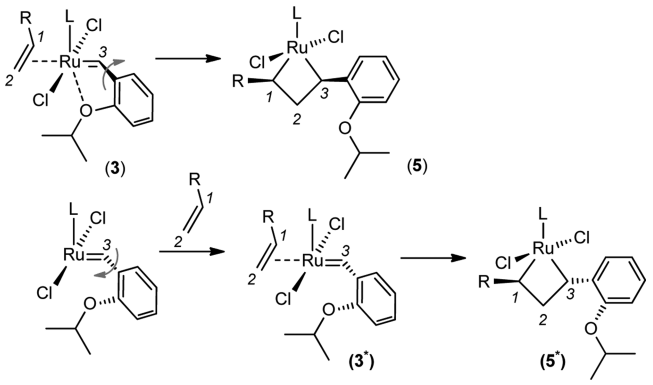

Figure 9. Alternative mechanisms leading to cis (**5**) and trans (**5***) MCBs.

Thus, in this alternative mechanism, initiation of the precatalyst occurs by a dissociative, rather than by an interchange mechanism, followed by binding of the substrate to form a low energy η-complex and MCB, the rate determining step being the initial dissociation of the precatalyst. For both GH2 (**I**) and Grela (**II**), this initiation step, which could involve either of the two closely spaced TSs (**14-TS**, **15-TS**) which we have found, has a barrier which is still greater by ∼2−6 kcal mol^{-1} than for the rate determining step (MCB formation) for the reaction which proceeds via an interchange mechanism. Thus, we find the latter mechanism to be the preferred one, at least for an EVE substrate.

A second alternative pathway is the associative mechanism which we[5] and Solans-Monfort[29] have previously investigated. In contrast to the interchange mechanism which involves concurrent movement of alkene and alkylidene, this mechanism involves movement of the alkene and one chlorine ligand, to give a η-complex having the chlorine ligands in a cis, rather than a trans configuration, with the position of the alkylidene little changed. We have previously reported a study of this associative mechanism with an ethene substrate[5] and found that the barrier to the formation of the initial η-complex was at 21.6 kcal mol^{-1} compared to 18.2 kcal mol^{-1} for the interchange mechanism. For a larger substrate Solans-Monfort[29] has found that for an associative mechanism, the corresponding MCB lies in a shallow well, 3.6 kcal mol^{-1} below the TS leading to its formation, which is the rate determining step.

For the corresponding associative mechanism for EVE and (**I**), we find that the MCB is also of high energy, 15.4 kcal mol^{-1}, above the van der Waals complex, the barrier to its formation from the η-complex being 19.2 kcal mol^{-1}, which is slightly (1 kcal mol^{-1}) lower than the corresponding barrier (20.2 kcal mol^{-1}) for the interchange mechanism. We find that for an associative mechanism the barrier for formation of the first η-complex from the initial van der Waals complex is 16.6 kcal mol^{-1}, compared to the value of 14.0 kcal mol^{-1} for the interchange mechanism (Figure 7). Thus, MCB formation is again rate determining.

However, compared to the interchange mechanism, we find that the barriers for the associative mechanism are more solvent dependent. The calculations in this paper have been carried out for ε = 8.93 (dichloromethane). We find that a smaller dielectric now favors the interchange, rather than the associative mechanism, Thus, for a dielectric (ε =1), the rate determining barrier to MCB formation is 19.3 and 23.1 kcal mol^{-1} respectively for the interchange and associative mechanisms. A similar effect is found for toluene (ε = 2.37), with barriers of 19.7 and 21.0 kcal mol^{-1} for the interchange and associative mechanisms respectively. Thus, our calculations predict that an interchange mechanism is favored in toluene, but in dichloromethane, an associative mechanism is favored. We note that the kinetic studies of Plenio et al.[17] were indeed carried out in toluene. In view of these small differences in the computed barriers, and bearing in mind the accuracy of DFT[24] and implicit solvent models,[38] we believe that it is difficult to distinguish between the interchange and the associative mechanisms, which could well depend upon solvent.

DISCUSSION

Although the basic mechanism of Grubbs−Hoveyda precatalysts is well-known, the nature of the initiation step, and which step in the reaction sequence is rate determining are still open to question. Our present study extends our previous preliminary communication[5] and complements the extensive studies of Solans-Monfort et al.[29] When taken together these studies show that conformational changes along the pathway must be considered, and can give rise to different PES surfaces which may be so close in energy so as to pose a challenge to present computational strategies, which are DFT based. In the present paper, we have explored some, but by no means all, of these conformational aspects.

Our calculations have shown that although the general features of the PES are similar for the three precatalysts and four substrates studied herein, there are quantitative differences between the different substrates which have important implications for the kinetic behavior of these systems. As far as the initiation step is concerned, we have located two alternative TSs for the dissociative mechanism, with barriers in the range 21−25 kcal mol^{-1} which are consistently higher than for the alternative interchange mechanism for all precatalysts and substrates when the reactant is taken to be a van der Waals complex. The dissociative mechanism also has, as expected, a very small and positive entropy of activation, while the interchange mechanism has a substantial negative entropy of activation, in agreement with experiment.

We have studied in detail the PESs for the reaction which proceeds via the interchange mechanism, noting that the pathway for the associative mechanism is close in energy, and may in some cases be preferred. The three TSs leading to the formation of the final η^2-complex (**7**) are quite close in energy for the ethene substrate. For the propene substrate, the TS leading to the formation of (**7**) is considerably below the first two TSs, while for EVE, it is lower still with the TS leading to formation of the MCB (**5**) being well above the other two. We have rationalized these trends in terms of the relative stability of the η^2-complex (**7**). In the case of propene, this final complex (**4**) which gives rise to the ethylidene is about 6 kcal mol^{-1} more stable than in the case of ethene. We associate this

dx.doi.org/10.1021/cs400164w | ACS Catal. 2013, 3, 1929−1939

stabilization with the hyperconjugation of the methyl group to the Ru=C moiety, which is however considerably larger than the expected value of 3 kcal mol^{-1}.[39] We may use the isodesmic reaction (Scheme 4) to quantify the difference in methyl

Scheme 4. Isodesmic Reaction Used to Quantify Methyl Hyperconjugation in the η^2-Complex (7)

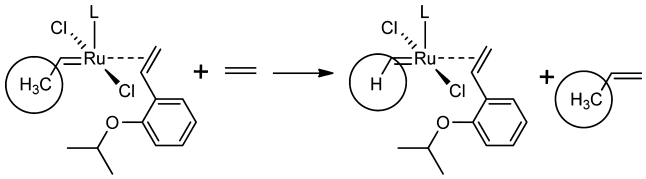

hyperconjugation in propene and in the η^2-complex (7). The free energy calculated for this reaction is 3.8 kcal mol^{-1}. Thus, if we take the hyperconjugation of propene to be ~3 kcal mol^{-1} we expect the hyperconjugation in the complex (7) to be ~7 kcal mol^{-1} which is close to the 6 kcal mol^{-1} value which we find. This additional hyperconjugation compared to that of propene is reflected in the corresponding geometric parameters (Supporting Information, Table S3).

In the case of the EVE substrate, the η^2-complex (7) is considerably more stable than in the case of propene, being about 2 kcal mol^{-1} below the initial reactants (**1**), whereas in propene, complex (7) is 8 kcal mol^{-1} above the reactant structure (**1**) (Figures 4 and 7). The stability of (7) in the case of EVE is reflected in a reduction in the O−C bond length from 1.35 Å in the isolated substrate to 1.32 Å in the η^2-complex (7).

Solans-Monfort et al. have highlighted their finding that the Ru···O distance is not the determining factor for the catalytic activity, and the importance of π delocalization between the phenyl and the carbene in the precatalyst.[40] We also find quite small changes in the Ru···O distance for GH2 (**I**), (**II**), and (**III**) (Supporting Information, Table S1), these values being within 0.1 Å. They have also studied the free energy profile for the dissociative and interchange mechanisms for the activation of GH2(**I**) by *N*,*N*-diallylmethanesulfonamide and by 1-allyloxy-2-propyne.[29] They find that if the reactants are taken to be two separate molecules, then the dissociative mechanism is preferred by ~4 kcal mol^{-1} . However in the work presented here where the reactant is taken to be the van der Waals complex ("supermolecule") of precatalyst and substrate we find the interchange mechanism to be preferred by ~8 kcal mol^{-1} (for EVE). As noted by Solans-Monfort et al. such differences arise since the use of a "supermolecule" favors the interchange mechanism as it does not include the entropy cost of the associative process, which is present when the reactant is taken to be two separate molecules.

We have investigated the effect of taking the reactant to be two separate molecules, EVE and GH2(**I**). The values of ΔG and ΔH for the formation of the van der Waals complex were computed to be 9.3 and −2.9 kcal mol^{-1} respectively, illustrating the loss of entropy of the individual molecules on formation of the complex. However, our estimates of the entropy contributions are for a gas phase model and do not include the effect of solvent, and including the solvent has proved difficult as well as controversial. It is generally agreed that the gas phase estimates provide an upper bound to the entropy loss, but the actual value is considerably smaller. Irudayam and Henchman[41] have discussed this problem in detail and conclude that the use of gas phase values may overestimate the entropy loss by up to a factor of ~2. We cannot be sure of the true value in solution but have reduced the entropy loss by this amount to provide some insight into its effect. Thus, the scaled ΔG value is now 3.2 rather than 9.3 kcal mol^{-1}. If we now refer the corresponding PES (Figure 7) for the interchange mechanism to this new zero of energy, **2-TS** and **4-TS** are now at 19.0 and 23.3 kcal mol^{-1}. The rate determining step for this interchange mechanism, that of MCB formation, now has essentially the same barrier as that for the dissociative mechanism where **15-TS** is at 22.6 kcal mol^{-1}. However, an accurate comparison of the energetics of the interchange and dissociative mechanisms is made difficult by the entropy problem. We further note that as suggested by Solans-Monfort et al., the "supermolecule" approach may be more appropriate for more concentrated solutions, so that the favored pathway may be concentration dependent. Of the two subsequent steps, MCB formation and decomposition, we are in agreement with Solans-Monfort et al. that MCB formation is the more energetic.

In the case of all three substrates (ethene, propene, and EVE) we have been unable to locate a TS for the final step in the reaction sequence, that of the dissociation of the second η^2-complex (7) to give 14e ruthenium species, although we have found TSs corresponding to rotation of the alkylidene ligand leading to a weakening of the η^2-bond. However, this weakening does not lead to dissociation, but rather to rotation

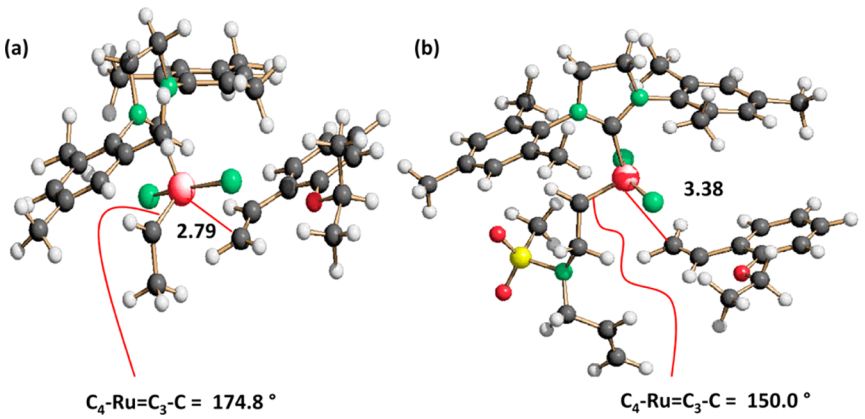

Figure 10. Transition structures for alkylidene rotation in final η^2-complex (7), showing Ru−C η^2-bond (distance in Å): (a) for propene as substrate, where the η^2-bond is weakened but not broken and (b) for *N*,*N*-diallylmethylsulfonamide, labeled TS(4E$_D$-4F),[29] where the η^2-bond is broken.

dx.doi.org/10.1021/cs400164w | *ACS Catal.* 2013, 3, 1929−1939

of the alkylidene ligand, and recapture of the styrene. This behavior is somewhat different from that reported by Solans-Monfort et al.[29] for the larger substrates, *N*,*N*-diallylmethanesulfonamide and 1-allyloxy-2-propyne where TSs leading to dissociation of the second η^2-complex have been located. Examination of the reported TSs for these large ligands shows that they do resemble the ones we have located and correspond to rotation of the alkylidene ligand which is much bulkier than those we have considered (Figure 10). However, the distance between the ruthenium and the terminal carbon of the olefin is considerably greater for the bulkier ligand leading to the η^2-bond being broken, rather than just weakened, so that the rebinding of the styrene, which we find here for smaller ligands, does not occur.

The metathesis reaction of 2-butene with **G2** benzylidene catalyst has been studied computationally by Benitez et al.[42] who found that MCB decomposition is the rate determining step, whereas for **GH2** precatalysts we find that MCB formation is rate determining. To further compare the mechanism of **G2** and **GH2** catalysts we have studied the interchange mechanism whereby **G2** is activated by ethene in an analogous reaction to those studied for **GH2**. We find similar energetics to those for **GH2** (Figure 11), with the

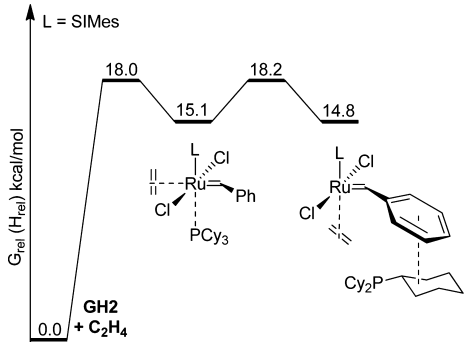

Figure 11. Partial PES for the initiation of **G2** with ethene.

barriers leading to the six-coordinate ethene η^2-complex being close to 18 kcal mol^{-1}. Webster[43] has studied an associative intermolecular pathway for ethene exchange in MCBs after Piers et al.[33] In the DFT study, the energetics of binding ethene to an MCB to form six-coordinate intermediate were also found to be feasible ($\Delta G^{\ddagger}$ = 16.6 kcal mol^{-1} and ΔG = 14.2 kcal mol^{-1} at the PBE level of theory). It may therefore even be possible, for relatively unhindered olefins, to avoid high energy free 14e ruthenium complexes throughout the cycle.

In our comparison with experiments with precatalysts **I** and **II**, where EVE is the substrate, we find excellent agreement between our predicted barriers for MCB formation and those from our experimental kinetic data, and in particular we predict the small change found in the barrier upon NO_2 substitution. Thus, electronic effects alone exert a small influence over the rate at which the precatalyst enters the cycle, suggesting that precatalyst design strategies based on electronic perturbation appear to have already been exhausted by Grela as there are few better electron withdrawing groups than NO_2.

We also find that the predicted barriers for EVE and 1-hexene are close, in accord with the experimental findings of Plenio et al.[17] and that the barrier predicted for our rate determining step, which is in excellent agreement with experiment, and in addition is similar to our predicted barrier for initiation by a dissociative mechanism. For GH2(**I**) and Grela (**II**) with an EVE substrate we find an alternative mechanism in which the rate determining step is the initial dissociation of the precatalyst leading to the trans form of the MCB. We find that the rate determining barrier for this alternative mechanism is 2−6 kcal mol^{-1} above that for the reaction which proceeds via an interchange initiation mechanism. For other precatalysts and substrates this difference could well be smaller, or indeed reversed in sign, leading to the observation of both dissociative and interchange mechanisms as reported by Plenio et al.[17]

However, calculations for our preferred mechanism predict that the rate determining step reaches much further into the pathway than the initial interchange step. This is entirely consistent with our predictions of the UV/visible spectra of the intermediates along the reaction pathway which strongly suggest that intermediates other than the initial η^2-complex are being monitored. Thus, taken overall our predictions are sufficiently robust to allow us to predict the behavior of new catalysts and substrates and hence to contribute to catalyst design.

CONCLUSIONS

In conclusion, we have provided further insight into the mechanism of precatalyst initiation in metathesis chemistry, which may have useful applications in the design of new precatalysts and in the understanding of the interplay between substrate structure and reactivity. Clearly, steps beyond the initial binding of the substrate have a degree of control over the reaction rate, with the barriers for MCB formation being competitive with those for alkene binding via the interchange or associative pathway, which we still believe represents the preferred mechanism for precatalyst initiation, at least for the substrates and precatalysts studied herein.

In agreement with detailed experimental studies by the Piers and Grubbs research groups, the pathways in which α,α'-substituted MCBs are formed are more favorable than ones in which α,β-substituted MCBs arise; the former leads to the production of a new alkylidene and loss of the styrene ligand, while the latter produces a methylidene complex (in the case of terminal olefins) and a β-substituted styrene compound.

Interestingly, an associative mechanism for the initiation of **G2** is found to be energetically feasible for small alkenes such as ethene; we were unable to probe this pathway experimentally, but the computational result suggests that the role of ethene may be worthy of more detailed investigation.

The results documented herein provide new insight into the initiation mechanism of **GH2** and analogues, and lay the groundwork for further investigations in this area. These calculations are likely to be of considerable use to those designing new systems, as they allow the initiation behavior to be investigated without the need for time-consuming and expensive preparation and testing of a library of complexes.

ASSOCIATED CONTENT

Supporting Information

Kinetic procedures and results. Computed energies, bond lengths, and Cartesian coordinates for the structures studied. This material is available free of charge via the Internet at http://pubs.acs.org.

AUTHOR INFORMATION

Corresponding Author

*E-mail: ian.hillier@manchester.ac.uk (I.H.H.), jonathan.percy@strath.ac.uk (J.M.P).

Present Address

[‖]EaStCHEM, School of Chemistry, University of St. Andrews, Purdie Building, North Haugh, St. Andrews, Fife, KY16 9ST, U.K.

Notes

The authors declare no competing financial interest.

ACKNOWLEDGMENTS

We thank AstraZeneca (Industrial CASE Studentship to D.J.N.) and the EPSRC for funding this work (Initiative in Physical Organic Chemistry 2: EP/G013160/1 and EP/G013020/1). We thank a reviewer for suggesting the use of the CAM-B3LYP functional.

REFERENCES

(1) Nolan, S. P.; Clavier, H. *Chem. Soc. Rev.* **2010**, *39*, 3305.
(2) Hoveyda, A. H.; Zhugralin, A. R. *Nature* **2007**, *450*, 243.
(3) Getty, K.; Delgado-Jaime, M. U.; Kennepohl, P. *J. Am. Chem. Soc.* **2007**, *129*, 15774.
(4) Hillier, I. H.; Pandian, S.; Percy, J. M.; Vincent, M. A. *Dalton Trans.* **2011**, *40*, 1061.
(5) Ashworth, I. W.; Hillier, I. H.; Nelson, D. J.; Percy, J. M.; Vincent, M. A. *Chem. Commun.* **2011**, *47*, 5428.
(6) Broggi, J.; Urbina-Blanco, C. A.; Clavier, H.; Leitgeb, A.; Slugovc, C.; Slawin, A. M. Z.; Nolan, S. P. *Chem.—Eur. J.* **2010**, *16*, 9215.
(7) Benitez, D.; Tkatchouk, E.; Goddard, W. A. *Organometallics* **2009**, *28*, 2643.
(8) Sanford, M. S.; Love, J. A.; Grubbs, R. H. *J. Am. Chem. Soc.* **2001**, *123*, 6543.
(9) Sanford, M. S.; Ulman, M.; Grubbs, R. H. *J. Am. Chem. Soc.* **2001**, *123*, 749.
(10) Samojlowicz, C.; Bieniek, M.; Grela, K. *Chem. Rev.* **2009**, *109*, 3708.
(11) Vougioukalakis, G. C.; Grubbs, R. H. *Chem. Rev.* **2010**, *110*, 1746.
(12) Love, J. A.; Sanford, M. S.; Day, M. W.; Grubbs, R. H. *J. Am. Chem. Soc.* **2003**, *125*, 10103.
(13) Barbasiewicz, M.; Michalak, M.; Grela, K. *Chem.—Eur. J.* **2012**, *18*, 14237.
(14) Grela, K.; Harutyunyan, S.; Michrowska, A. *Angew. Chem., Int. Ed.* **2002**, *41*, 4038.
(15) Michrowska, A.; Bujok, R.; Harutyunyan, S.; Sashuk, V.; Dolgonos, G.; Grela, K. *J. Am. Chem. Soc.* **2004**, *126*, 9318.
(16) Vorfalt, T.; Wannowius, K. J.; Plenio, H. *Angew. Chem., Int. Ed.* **2010**, *49*, 5533.
(17) Thiel, V.; Hendann, M.; Wannowius, K. J.; Plenio, H. *J. Am. Chem. Soc.* **2012**, *134*, 1104.
(18) Vougioukalakis, G. C.; Grubbs, R. H. *J. Am. Chem. Soc.* **2008**, *130*, 2234.
(19) Barbasiewicz, M.; Blocki, K.; Malinska, M.; Pawlowski, R. *Dalton Trans.* **2013**, *42*, 355.
(20) Zhao, Y.; Truhlar, D. G. *J. Chem. Phys.* **2006**, *124*, 224105.
(21) Zhao, Y.; Truhlar, D. G. *J. Chem. Phys.* **2006**, *125*, 194101.
(22) Zhao, Y.; Truhlar, D. G. *Acc. Chem. Res.* **2008**, *41*, 157.
(23) Zhao, Y.; Truhlar, D. G. *Org. Lett.* **2007**, *9*, 1967.
(24) Pandian, S.; Hillier, I. H.; Vincent, M. A.; Burton, N. A.; Ashworth, I. W.; Nelson, D. J.; Percy, J. M.; Rinaudo, G. *Chem. Phys. Lett.* **2009**, *476*, 37.
(25) Frisch, M. J.; Trucks, G. W.; Schlegel, H. B.; Scuseria, G. E.; Robb, M. A.; Cheeseman, J. R.; Scalmani, G.; Barone, V.; Mennucci, B.; Petersson, G. A.; Nakatsuji, H.; Caricato, M.; Li, X.; Hratchian, H. P.; Izmaylov, A. F.; Bloino, J.; Zheng, G.; Sonnenberg, J. L.; Hada, M.; Ehara, M.; Toyota, K.; Fukuda, R.; Hasegawa, J.; Ishida, M.; Nakajima, T.; Honda, Y.; Kitao, O.; Nakai, H.; Vreven, T.; Montgomery, J. A.; Peralta, J. E.; Ogliaro, F.; Bearpark, M.; Heyd, J. J.; Brothers, E.; Kudin, K. N.; Staroverov, V. N.; Kobayashi, R.; Normand, J.; Raghavachari, K.; Rendell, A.; Burant, J. C.; Iyengar, S. S.; Tomasi, J.; Cossi, M.; Rega, N.; Millam, J. M.; Klene, M.; Knox, J. E.; Cross, J. B.; Bakken, V.; Adamo, C.; Jaramillo, J.; Gomperts, R.; Stratmann, R. E.; Yazyev, O.; Austin, A. J.; Cammi, R.; Pomelli, C.; Ochterski, J. W.; Martin, R. L.; Morokuma, K.; Zakrzewski, V. G.; Voth, G. A.; Salvador, P.; Dannenberg, J. J.; Dapprich, S.; Daniels, A. D.; Farkas; Foresman, J. B.; Ortiz, J. V.; Cioslowski, J.; Fox, D. J. *Gaussian 09*, Revision B.01; Gaussian Inc.: Wallingford, CT, 2009.
(26) Hansen, S. M.; Rominger, F.; Metz, M.; Hofmann, P. *Chem.—Eur. J.* **1999**, *5*, 557.
(27) Yanai, T.; Tew, D. P.; Handy, N. C. *Chem. Phys. Lett.* **2004**, *393*, 51.
(28) Dev, P.; Agrawal, S.; English, N. J. *J. Phys. Chem. A* **2012**, *117*, 2114.
(29) Nunez-Zarur, F.; Solans-Monfort, X.; Rodriguez-Santiago, L.; Sodupe, M. *Organometallics* **2012**, *31*, 4203.
(30) In a literature report, the *phosphane-bound* methylidene was preferred over the *phosphane-bound* benzylidene (K_{eq} = 8.7), but this work considers the formation of a four co-ordinate 14e complex from a five co-ordinate 16e species. In a synthetic reaction, the 14e species thus generated would proceed to react with the alkene present in solution. See Lane, D. R.; Beavers, C. M.; Olmstead, M. M.; Schore, N. E. *Organometallics* **2009**, *28*, 6789.
(31) The σ_p^+ constant for *para* MeO is −0.78, whereas the value for *para* NO_2 is +0.79. Stronger donors are *para* Me_2N at −1.7 and *para* O- at −2.3. See Hansch, C.; Leo, A.; Taft, R. W. *Chem. Rev.* **1991**, *91*, 165.
(32) Romero, P. E.; Piers, W. E. *J. Am. Chem. Soc.* **2005**, *127*, 5032.
(33) Romero, P. E.; Piers, W. E. *J. Am. Chem. Soc.* **2007**, *129*, 1698.
(34) van der Eide, E. F.; Piers, W. E. *Nat. Chem.* **2010**, *2*, 571.
(35) Wenzel, A. G.; Grubbs, R. H. *J. Am. Chem. Soc.* **2006**, *128*, 16048.
(36) Wenzel, A. G.; Blake, G.; VanderVelde, D. G.; Grubbs, R. H. *J. Am. Chem. Soc.* **2011**, *133*, 6429.
(37) Keitz, B. K.; Grubbs, R. H. *J. Am. Chem. Soc.* **2011**, *133*, 16277.
(38) Takano, Y.; Houk, K. N. *J. Chem. Theory Comput.* **2004**, *1*, 70.
(39) Skinner, H. A.; Pilcher, G. *Quart. Rev. Chem. Soc.* **1963**, *17*, 264.
(40) Solans-Monfort, X.; Pleixats, R.; Sodupe, M. *Chem.—Eur. J.* **2010**, *16*, 7331.
(41) Irudayam, S. J.; Henchman, R. H. *J. Phys.Chem. B* **2009**, *113*, 5871.
(42) Benitez, D.; Tkatchouk, E.; Goddard, W. A. *Chem. Commun.* **2008**, 6194.
(43) Webster, C. E. *J. Am. Chem. Soc.* **2007**, *129*, 7490.